MT-Pallantia Publisher
Journal of Science with Technological Applications
ISSN: 0719-8647

Extraction and characterization of biogenic hydroxyapatites obtained from fish scales of the Cachama, Black Tilapia and Red Tilapia species

Sara L. Hernández [1], Manuel Palencia [1], Andrés F. Chamorro [2,3]

[1] *Research Group with Technological Applications (GI-CAT), Chemistry Department, Universidad del Valle, Cali-Colombia.*
[2] *Mindtech Research Group (Mindtech-RG), Mindtech S.A.S., Cali-Colombia.*
[3] *Research Group of Electrochemistry and Environment (GIEMA), Faculty of Basic Sciences, Universidad Santiago de Cali, Cali – Colombia.*

Corresponding Author: Manuel Palencia. E-mail: manuel.palencia@correounivalle.edu.co

Graphical Abstract

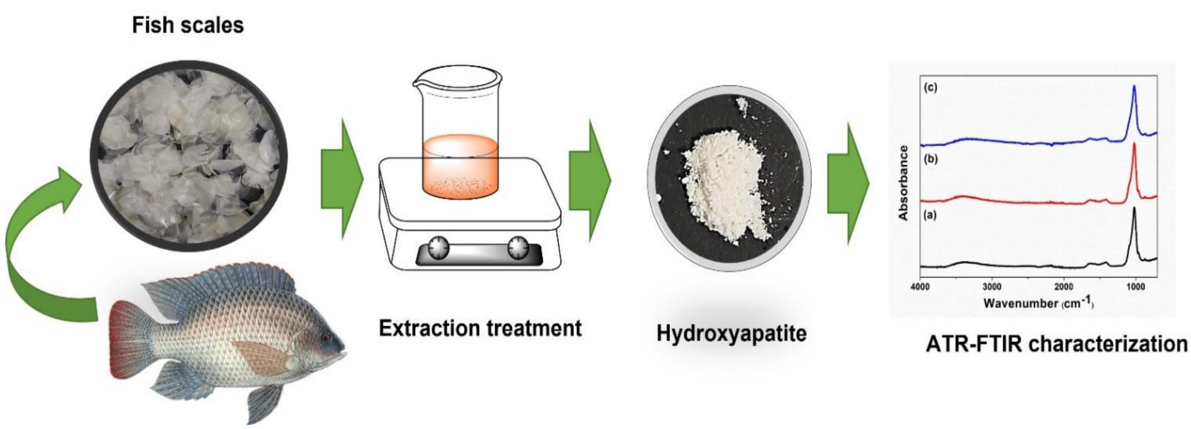

Abstract. Hydroxyapatite (HAP) is the primary mineral component of human bone tissue, making it a valuable material for bone repair due to its biocompatibility, osteoconductivity, rigidity, and hardness. HAP can be sourced from biological materials such as fish scales, aligning with the growing interest in sustainable and ecological production strategies. In Colombia, fish production significantly increased between 2011 and 2020, yielding 179,351 tons of various native species, with Tilapia and Cachama being particularly significant. However, a substantial portion of this production, including filleting remains, skin, fins, skeletons, heads, viscera, and scales, is considered waste but could be repurposed for valuable by-products like HAP. In this study, fish scales from Cachama (CH, *Piaractus brachypomus*), Black Tilapia (BT, *Oreochromis niloticus*), and Red Tilapia (RT, *Oreochromis sp.*) were used to extract biogenic HAP. The scales were treated with an alkaline method, and the percentage of HAP obtained was evaluated. The total percentage of HAP followed the trend: BT (59.0 ± 1.8 %) > RT (47.6 ± 1.7 %) > CH (29.8 ± 1.2 %), indicating that the HAP content varies depending on the fish species. The extracted HAP was characterized using ATR-FTIR spectroscopy and identified as type B carbonated HAP (HAC-B). Additionally, the HAP particles were found to be on the nanometric scale, enhancing their potential biomedical applications.

Keywords: Hydroxyapatite, *Piaractus brachypomus, Oreochromis niloticus, Orechromis sp*.

Cite as: Hernández S.L., Palencia M., Chamorro A.F. Extraction and characterization of biogenic hydroxyapatites obtained from fish scales of the Cachama, Black Tilapia and Red Tilapia species. J. Sci. Technol. Appl., 21, 2024 (in JSTA 2026), Art-122, 1-6.
https://doi.org/10.34294/j.jsta.26.21.122

Accepted: 2024-08-02 | Published: 2024-08-25 | Paper Number: 122 (STEM) | Research Article

1. Introduction

Hydroxylapatite (HAP, $Ca_{10}(PO_4)_6(OH)_2$ is an apatite biocrystal composed of calcium, phosphorus, and hydrogen. However, natural HAP crystals often contain traces of sodium, chlorine, carbonates, and magnesium, which means they are not considered pure apatite (Techochatchawal, 2009). his mineral is the main component of bone tissue in humans and animals, accounting for 99 % of the body's calcium, 80 % of its total phosphorus, and making up 96 % of tooth enamel (Bermúdez et al., 2021). HAP exhibits multiple properties, such as biocompatibility, osteoconduction, mechanical rigidity and hardness, making it a promising material for use in the dental industry and biomedical prostheses (García and Reyes, 2006). For example, HAP has been explored for repairing hard tissue, offering an alternative to autografts and allografts by promoting osseointegration (Santos et al., 2001).

Recently, nanoscale HAP has been investigated for various applications, including the adsorption of heavy metals like Pb, Cu, and Cd to remove contaminants (Nayak and Brij, 2021). Additionally, it has been explored for controlled drug release; for instance, nano-HAP was used to deliver doxorubicin (DOX), an anticancer drug. The research demonstrated that these nanomaterials could be intercalated with DOX, releasing the drug in a controlled manner in both *in vitro* and in *vivo* (animal models) assays (Kundu et al., 2013). Another recent application of HAP is its use as a surface for forming electrochemical biosensors (Hartati et al., 2022). For example, HAP nanoparticles modified with graphite have been utilized for the electrochemical detection of DNA (Erdem and Congur, 2018).

Given the diverse applications mentioned above, there is a growing need for cost-effective HAP with high performance. Several methodologies have been reported for the synthesis of HAP, including dry methods (solid-state and mechanochemical), wet methods (electrochemical, chemical precipitation, sol-gel, hydrothermal, and sonochemical), and high-temperature processes (combustion, pyrolysis, microwave, and biosynthesis) (Hartati et al., 2022). However, most of these methodologies rely on phosphate and calcium salts for HAP formation, which increases production costs and limits broader application. There is significant interest in developing more sustainable and ecological production strategies to address this issue, including using renewable raw materials (Sierra, 2021). As a result, various biological sources have been explored for HAP synthesis, including mammalian bone remains, bird eggshells, coral remains, and fish bones and scales (Aquino and Linares, 2020).

Fish scales have become a promising alternative raw material for HAP production due to their widespread availability as a waste product. Globally, about 40 % of fish farming is intended for human consumption, while the remaining 60 % is generally considered waste (Chalamaiah et al., 2012). This waste is often used for low-value applications such as animal feed, fishmeal, and fertilizer (Sierra, 2021). The composition of these by-products is approximate: filleting remains (15-20 %), skin and fins (1-3 %), skeletons (9-15 %), heads (9-12 %), viscera (12-18 %), and scales

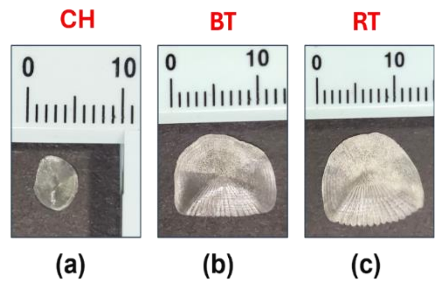

Figure 1. Digital photography of representative scales of CH, BT, and RT.

(5 %) (Shen et al., 2018). In Colombia specifically, aquaculture production increased by 216 % between 2011 and 2020, producing 179,351 tons of tilapia, trout, cachama, shrimp, and other native species. Tilapia accounted for 58 % of this production, and cachama accounted for 19 %, making them the most cultivated species in the country (Ministry of Agriculture and Rural Development, 2020). Considering the aforementioned information, it is estimated that in 2020, around 8,703 tons of scale waste were generated in Colombia. Therefore, fish scales can be utilized as sources of commercially valuable products, such as HAP. In this study, waste fish scales from species with high production in Colombia, including Cachama (CH, *Piaractus brachypomus*), Black Tilapia (BT, *Oreochromis niloticus*), and Red Tilapia (RT, *Oreochromis sp.*), were used for the extraction of biogenic HAP. The extracted HAP was characterized using Attenuated Total Reflectance-Fourier Transform Infrared Spectroscopy (ATR-FTIR), Dynamic Light Scattering (DLS), and Thermogravimetric Analysis (TGA).

2. Methodology

2.1. Materials

Sodium dodecyl sulfate (SDS, $NaC_{12}H_{25}SO_4$, 99 %), hydrochloric acid (HCl, 37 %), isopropanol (C_3H_8O, 99.5%), and sodium hydroxide (NaOH, 97 %) were purchased from Sigma-Aldrich. Distilled water was used to prepare the aqueous solutions of HCl, SDS, and NaOH, as well as to clean the scales.

2.2. Scales collection

CH, RT, and BT samples were manually collected at the Las Brisas fish farm, located along the Buga-Ginebra Road in Ginebra, Valle del Cauca. The scales were removed by scraping the fish skin against the direction of scale growth using a spoon, and each set of scales was placed in a labeled bag. The CH scales were collected with a thin knife, similarly placed in labeled bags, and then frozen until further use.

2.3. HApNPs extraction

The procedure for obtaining HAP was based on a modification of the methodology proposed by Pon-On et al., (2016). First, the co-

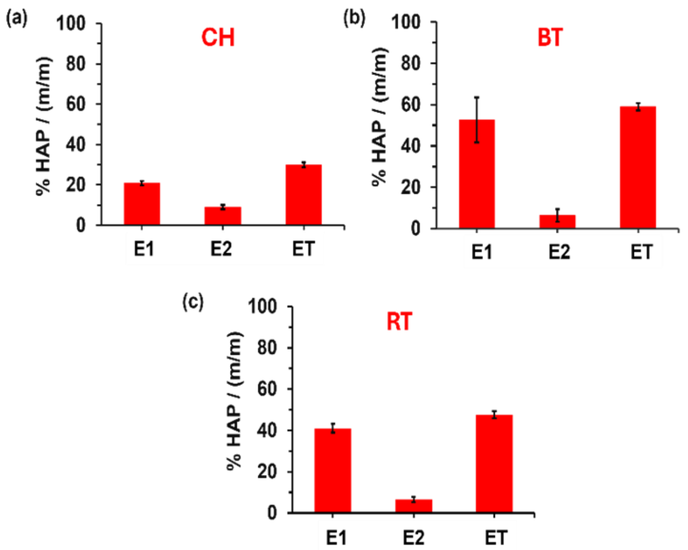

Figure 2. Percentage of HAP extracted from: a) CH, b) BT, and c) RT scales. E1, E2, and ET correspond to extraction 1, extraction 2 and total extraction (E1+E2), respectively.

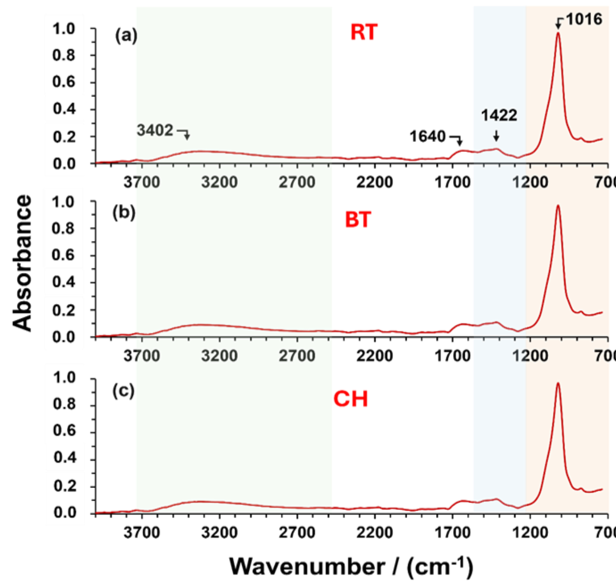

Figure 3. ATR-FTIR spectrum of HAP extracted from: (a) RT, (b) BT and (c) CH.

llected scales were thawed and dried. Then, the scales were washed with a 5 % (w/v) SDS solution, submerged in a 1:10 ratio in the solution, and stirred for 24 hours. They were subsequently rinsed thoroughly with water until the foam disappeared, then rinsing with distilled water and drying in an oven at 60 °C. The pre-treated fish scales were then immersed in a 1:10 ratio in a 4 % HCl solution with constant stirring at room temperature for 24 hours. After this, 0.5 M NaOH was added to the solution to create a suspension rich in HAP, maintaining the pH above 7, at which point the HAP precipitates. The HAP was then collected by filtration, followed by drying in an oven at 60 °C for 48 hours. The product obtained from this process is referred to as extraction 1 (E1). The percentage of HAP content (% HAP) was calculated using **Equation 1**:

$$\% \text{ HAP} = \frac{(m_{HAP-FP} - m_{FP})}{m_i} \times 100 \qquad (1)$$

where m_i, m_{FP}, and m_{HAP-FP} represent the mass of the scales, dry filter paper, and dry filter paper with HAP after the filtration process, respectively. The remaining fish scales from the E1 process were subjected to a re-extraction process, resulting in a second HAP extraction, referred to as extraction 2 (E2). All extractions in this study were performed in triplicate.

2.4. HAP characterization

The HAP obtained from CH, RT, and BT scales were characterized using ATR-FTIR, TGA, and DLS. ATR-FTIR measurements were (Shimadzu), covering a range from 700 cm^{-1} to 4000 cm^{-1} at a resolution of 2 cm^{-1} per data point, with 16 scans for each HAP sample. The size of the HAP particles was analyzed using DLS with a Zetasizer Lab (Malvern), using isopropanol as the solvent to disperse the HAP materials. TGA analysis was performed with a thermogravimetric analyzer (SDT-Q600, TA Instruments). Approximately 10 mg of each HAP sample was heated from 25°C to 800°C at a constant heating rate of 10°C/min under a nitrogen flow of 20 mL/min.

3. Results and discussion

Fish scales are composed of hydroxyapatite and collagen, forming a composite structure. **Figure 1** illustrates the geometric differences between CH, BT, and RT fish scales. The CH scales exhibit a spherical shape, whereas both tilapia scales (BT and RT) have semi-circular geometric shapes, with the RT scales being larger than the CH scales. Consequently, the tilapia scales are expected to contain a higher amount of HAP compared to the CH scales. **Figure 2** illustrates the percentage of HAP obtained from CH, BT, and RT scales. The HAP was extracted using two processes (E1 and E2), with the combined total of both extractions represented as ET. The % HAP obtained in the first extraction followed the trend: BT (52.6 ± 10.8 %) > RT (41.0 ± 2.1 %) > CH (20.8 ± 1.0 %), indicating variations in HAP composition among the scales. Notably, the % HAP obtained in the first extraction is higher for all fish species than that in the second extraction. Additionally, the % HAP obtained in the second extraction (E2) was less than 10 % (w/w) for all species, suggesting that the reagents used in the extraction were insufficient to compensate for the quantity of product obtained.
The total % HAP obtained from the scales (ET) exhibited the same trend as observed in the first extraction (E1): BT (59.0 ± 1.8 %) >

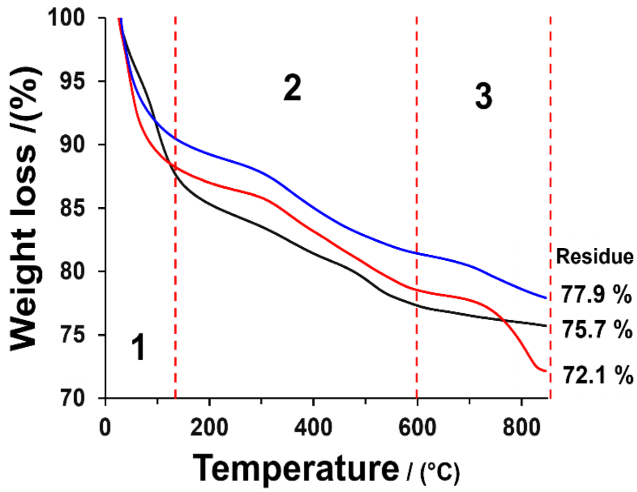

Figure 4. TGA analysis of HAP extracted from: CH (—), BT (—), and RT (—).

RT (47.6 ± 1.7 %) > CH (29.8 ± 1.2 %), indicating that BT scales have the highest % HAP. These results contrast with those reported by Zainol et al., (2017), who extracted 36 % HAP from BT scales using alkaline treatment and calcination at 1200°C for 2 hours. The discrepancy is likely due to differences in the extraction methods employed.

The HAP obtained from fish scales was characterized using ATR-FTIR (**Figure 3**). The spectra from all species displayed similar bands, indicating the presence of comparable functional groups in the HAP. An intense band at 1016 cm^{-1} was observed, corresponding to the stretching vibrations of the PO_4^{3-} functional group. In the region between 3000 and 3700 cm^{-1}, the spectra exhibited a characteristic stretching band for –OH of H_2O, with a maximum at 3402 cm^{-1} for the HAP from RT scales. Additionally, a band at 1640 cm^{-1} was attributed to H_2O trapped within the HAP crystals. A band at 1422 cm^{-1}, attributed to CO_3^{2-} vibration, suggests that the HAP obtained from all fish scales can be classified as carbonated HAP type B (HAC-B). This type is characterized by the substitution of PO_4^{3-} for CO_3^{2-} during the HAP precipitation process (Moreno et al., 2012; Pon-On et al., 2016). HAC-B has the molecular formula $Ca_{10-x}(PO_4)_{6-x}(CO_3)_x(OH)_{2-x}$; $(0 \leq x \leq 2)$ (Ochoa et al., 2021), where carbonate ions replace phosphate ions in the hydroxyls. This type of apatite is considered calcium-deficient, with the Ca/P concentration ratio varying from 1.67 to 1.33 (Yubao et al., 1994). HAC-B is noted for its high biodegradability, biocompatibility, osteoinduction, and osteoconduction, making it a promising material for biomedical applications (Botero, 2016; Ochoa et al., 2021). Therefore, the HAP obtained in this study can be utilized to form composite materials for biomedical applications due to its excellent biocompatibility.

The HAP materials were characterized by TGA to assess their thermal stability (see **Figure 4**). The analysis revealed three distinct weight loss regions for all extracted HAP. 1) First Region (25 – 130 °C): A weight loss of approximately 10 % was observed, attributed to the loss of adsorbed and/or entrapped water in the HAP crystals. 2) Second Region (130 – 600 °C): This weight loss is likely due to the decomposition of organic compounds within the HAP matrix, including collagen (Paul et al., 2017). Finally, 3) Third Region (above 600 °C): Weight loss in this region is attributed to the loss of hydroxyl groups and the degradation of carbonate ions into CO_2 (Aziz et al., 2022). The scales demonstrated varying thermal stabilities, with residues at 850 °C following the sequence: RT (77.9 %) > CH (75.7 %) > BT (72.1 %). This indicates that approximately 70 % of the material extracted from the scales (ET) corresponds to pure HAP.

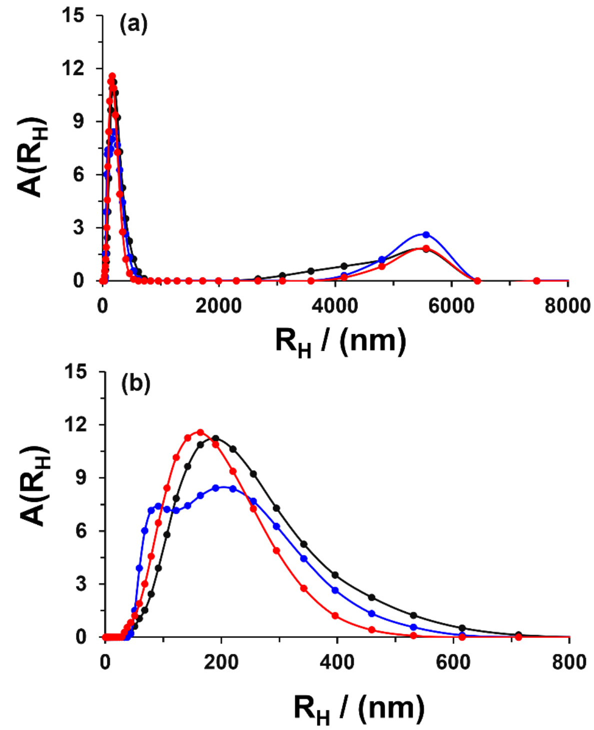

Figure 5. Amplitude of size distribution function $A(R_H)$ of HAP particles at a scattering angle of θ = 90° and 298.15 K: a) 0 – 8000 nm, and b) 0 – 800 nm. The HAP was extracted from CH (●), BT (●), and RT (●) fish scales.

Finally, the HAP extracted was analyzed by DLS. **Figure 5a** shows the size distribution profile of HAP particles using isopropanol as the solvent. All three HAP samples exhibited a bimodal size distribution characterized by slow and fast relaxation modes. The fast mode corresponds to individual HAP particles, while the slow mode represents aggregates of HAP particles, resulting in particle sizes of approximately 5500 nm, precipitating quickly from the solution. The individual HAP particles ranged from 50 to 600 nm (see **Figure 5**), with the maximum amplitude of particle size observed at 190 nm for both CH and BT samples.

In contrast, the HAP from RT had a slower size mode with a peak at 164 nm. This indicates that the HAP obtained from fish scales in this research has a nanometric size, broadening the potential applications of these materials. For instance, they could be used for the delivery and controlled release of drugs and active compounds as alternatives to conventional treatments. Additionally, these nanomaterials may serve as fertilizers due to their high phosphorus and calcium content, enhancing plant fertilization.

4. Conclusions

HAP derived from CH, BT, and RT fish scales was obtained using an alkaline treatment method. The extraction process yielded the highest amount of HAP in the first cycle. Among the scales, CH showed the lowest HAP extraction efficiency (29.8 ± 1.2 %), while BT and RT scales exhibited extraction percentages greater than 47 %. ATR-FTIR analysis confirmed the presence of HAC-B in the structure, which is highly stable at elevated temperatures and has a particle size range between 50 and 600 nm. The carbonated HAP produced in this research investigation was characterized by its biocompatibility, making it suitable for biomedical and pharmaceutical applications. Specifically, HAC-B compounds could be used for the immobilization and transportation of active compounds.

Conflict interest. The authors declare that there is no conflict of interest.

Acknowledgements. The authors acknowledge Mindtech s.a.s., Universidad del Valle, Golden-Hammer Institute, the Ministry of Science, Technology, and Innovation for project 80740-467-2021, and the Colombian National Planning Department, specifically the General Royalties System (SGR) for project BPIN2020000100261.

References

1. Aquino A., Linares, C. F. (2020). Hidroxiapatita: síntesis y caracterización. Revista de Operatoria Dental y Biomateriales. 9 (3), 24-30.

2. Aziz, K., Mamouni, R., Azrrar, A., Kjidaa, B., Saffaj, N., Aziz, F. (2022). Enhanced biosorption of bisphenol A from wastewater using hydroxyapatite elaborated from fish scales and camel bone meal: A RSM@ BBD optimization approach. Ceramics International, 48(11), 15811-15823. https://doi.org/10.1016/j.ceramint.2022.02.119

3. Bermúdez, V. S., Huaman, K., Castañeda, J. A.; Landauro, C. V., Quispe, J., Tay, L. Y. (2021). Obtención De Hidroxiapatita a Través De Residuos Biológicos Para Injertos óseos Dentales. Revista Estomatológica Herediana. 31 (2), 111-116. https://doi.org/10.20453/reh.v31i2.3971.

4. Botero, Y. L. (2016). Hidroxiapatita carbonatada, una opción como biomaterial para implantes: una revisión del estado del arte. Revista Colombiana De Materiales. (8), 79–97. https://doi.org/10.17533/udea.rcm.26893

5. Chalamaiah, M., Dinesh, K. B., Hemalatha, R., Jyothirmayi, T. (2012). Fish protein hydrolysates: proximate composition, amino acid composition, antioxidant activities and applications: a review. Chemistry. 135 (4), 3020-3038. https://doi.org/10.1016/j.foodchem.2012.06.100.

6. Erdem, A., Congur, G. (2018). Hydroxyapatite nanoparticles modified graphite electrodes for electrochemical DNA detection. Electroanalysis, 30(1), 67-74. https://doi.org/10.1002/elan.201700462

7. García, M.V., Reyes, J. (2006). La hidroxiapatita, su importancia en los tejidos mineralizados y su aplicación biomédica. TIP Revista Especializada en Ciencias Químico-Biológicas. 9 (2), 90-95. Available in: http://www.scielo.org.mx/scielo.php?script=sci_arttext&pid=S1405-888X2006000200090&lng=es&tlng=es

8. Hartati, Y. W., Irkham, I., Zulqaidah, S., Syafira, R. S., Kurnia, I., Noviyanti, A. R., Topkaya, S. N. (2022). Recent advances in hydroxyapatite-based electrochemical biosensors: Applications and future perspectives. Sensing and Bio-Sensing Research, 38, 100542. https://doi.org/10.1016/j.sbsr.2022.100542

9. Kundu, B., Ghosh, D., Sinha, M. K., Sen, P. S., Balla, V. K., Das, N., Basu, D. (2013). Doxorubicin-intercalated nano-hydroxyapatite drug-delivery system for liver cancer: An animal model. Ceramics International, 39(8), 9557-9566. https://doi.org/10.1016/j.ceramint.2013.05.074

10. Ministerio de Agricultura y Desarrollo Rural. (2020). Acuicultura en Colombia. Available in: https://bit.ly/3K11CE0.

11. Moreno, K. J., Hernandez, C., Garcia, S, Arizmendi, A., Aguilera, D., (2012). Síntesis y caracterización de nanopartículas de hidroxiapatita carbonatada. Instituto Tecnológico de Orizaba (ITO).

12. Nayak, A., Brij B. (2021). Hydroxyapatite as an advanced adsorbent for removal of heavy metal ions from water: Focus on its applications and limitations. Materials Today: Proceedings, 46, 11029-11034. https://doi.org/10.1016/j.matpr.2021.02.149

13. Ochoa, M. I., López, M. E., Copete, H. (2021). Síntesis y caracterización de polvos de hidroxiapatita carbonatada tipo b con diferentes contenidos de carbonato. Revista Colombiana de Materiales, (17), 22–32. https://doi.org/10.17533/udea.rcm.n17a03

14. Paul, S., Pal, A., Choudhury, A. R., Bodhak, S., Balla, V. K., Sinha, A., Das, M. (2017). Effect of trace elements on the sintering effect of fish scale derived hydroxyapatite and its bioactivity. Ceramics International, 43(17), 15678-15684. https://doi.org/10.1016/j.ceramint.2017.08.127

15. Pon-On, W., Suntornsaratoon, P., Charoenphandhu, N., Thongbunchoo, J., Krishnamra, N., Tang, I. (2016). Hydroxyapatite from fish scale for potential use as bone scaffold or regenerative material. Materials Science and Engineering: C. 62, 183-189. https://doi.org/10.1016/j.msec.2016.01.051.

16. Santos, C. L., Luklinska, Z. B., Clarke, R. L., Davy, K. W. M. (2001). Hydroxyapatite as a filler for dental composite materials: mechanical properties and in vitro bioactivity of composites. Journal of Materials Science: Materials in Medicine, 12, 565-573. https://doi.org/10.1023/a:1011291723503

17. Shen, X., Zhang, M., Bhandari, B., Gao, Z. (2018). Novel technologies in utilization of byproducts of animal food processing: a review. Critical Reviews in Food Science and Nutrition. 59 (21), 3420-3430. https://doi.org/10.1080/10408398.2018.1493428.

18. Sierra, L. (2021). Revaloración de escamas y esqueletos de tilapia roja (*Oreochromis spp.)* para la obtención de péptidos bioactivos. Universidad de Antioquia, Colombia.

19. Techochatchawal, K., Therdthai, N., Khotavivattana, S. (2009). Development of calcium supplement from the bone of nile tilapia (*Tilapia nilotica*). Asian Journal of Food and Agro-Industry. 2 (4), 539-546.

20. Zainol, I., Adenan, N. H., Rahim, N. A., Jaafar, C. A. (2019). Extraction of natural hydroxyapatite from tilapia fish scales using alkaline treatment. Materials Today: Proceedings, 16, 1942-1948. https://doi.org/10.1016/j.matpr.2019.06.072

21. Yubao, L., Klein, C.P.A.T., Wijn, J., Van, S., Groot, K. (1994). Shape changes and phase transition of needle-like non-stoichiometric apatite crystals. Journal of Materials Science: Materials in Medicine. 5, 263–268. https://doi.org/10.1007/BF00122395.